Available online at www.sciencedirect.com

ScienceDirect

Advances in Space Research 64 (2019) 385–399

ADVANCES IN SPACE RESEARCH
(a COSPAR publication)

www.elsevier.com/locate/asr

Airglow imaging observations of some evolutionary aspects of equatorial plasma bubbles from Indian sector

O.B. Gurav [a], V.L. Narayanan [b], A.K. Sharma [a,c,*], R.N. Ghodpage [d], H.P. Gaikwad [a], P.T. Patil [d]

[a] *Space and Earth Science Laboratory, Department of Physics, Shivaji University, Kolhapur, India*
[b] *National Atmospheric Research Laboratory, Gadanki, India*
[c] *School of Physics, Shri Mata Vaisno Devi University, Katra Kakryal, Katra, J&K, India*
[d] *Medium Frequency Radar, Indian Institute of Geomagnetism, Shivaji University Campus, Kolhapur, India*

Received 2 January 2019; received in revised form 4 April 2019; accepted 6 April 2019
Available online 12 April 2019

Abstract

The ground-based all sky imager (ASI) is an advanced optical technique, capable of measuring the strong F-region nightglow in OI 630.0 nm emission from atomic oxygen. This emission is used to study the large-scale F-region plasma irregularities; called as Equatorial Plasma Bubbles (EPBs) which often disturbs the communication and navigation systems over low latitudes. The observations of OI 630.0 nm nightglow emission have been carried out from low latitude station Kolhapur (16.8°N, 74.2°E, 10.6° dip. lat.) using ASI during moonless nights for the period of 2011 to 2015. We have analyzed images recorded by ASI during this period and found some interesting features of EPBs on few nights (08 cases). This paper reports the analysis and the dynamics of EPBs features such as bifurcation, merging and detachment. The bifurcation in EPBs occurs before mid-night and extends to couple of hours towards dawn. Also, the secondary structures are seen as evolving features on the eastern wall of EPBs. In one of the case, the EPBs are seen to merge with each other due to their opposite tilts. Also, some EPBs detach due to unequal drifts along the meridian indicating the presence of strong latitudinal gradient in zonal neutral winds or altitudinal shear in zonal plasma drift which might be responsible for this detachment. In some cases we note that the EPBs shrink. Some of these features support the previous findings and some are new which needs further detailed investigation.

Keywords: All sky imager; EPBs evolution; Bifurcation; Merging; Detachments

1. Introduction

All sky imaging technique has been extensively used to study the ionospheric irregularities using nightglow emissions at different wavelengths such as OI 630.0 nm, OI 557.7 nm from low latitude station Kolhapur since last several years (Mukherjee et al., 1998). The dark patches in optical data of OI 630.0 nm emission is because of the depletion in plasma density as compared to the background plasma density of ionospheric bottomside F region which is the signature of equatorial plasma bubbles (EPBs). The EPBs associated with equatorial spared F (ESF) are known to be generated at the bottom side of equatorial F-region, through a fluid-type gradient instability called Rayleigh-Taylor instability (Zalesak et al., 1982). EPBs are aligned with the geomagnetic field lines and drifts eastward. Also they are tilted toward the west of the magnetic north-south direction (Taori and Sindhya 2014; Narayanan et al., 2017).

* Corresponding author at: School of Physics, Shri Mata Vaisno Devi University, Katra Kakryal, Katra, J&K, India.
E-mail addresses: aks_phy@unishivaji.ac.in, ashok.kumar@smvdu.ac.in (A.K. Sharma).

https://doi.org/10.1016/j.asr.2019.04.008
0273-1177/

The occurrence (Sharma et al., 2014, 2017), dimensions (Sharma et al., 2012) and zonal drift velocity (Nade et al., 2013, Gurav et al, 2018) of EPBs have been studied previously using all-sky imager (ASI) data of OI 630.0 nm emission from Kolhapur. These field-aligned irregularities (FAI's) have also been studied using VHF radar by several investigators from tropical regions (Patra et al., 2009, 2014; Dao et al., 2016). To study the dynamics of low latitude F region, many researchers have investigated the occurrence, morphology and zonal drift velocity of EPBs using satellite based and ground based data (Pimenta et al., 2001; Martinis et al., 2003; Immel et al., 2004; England and Immel, 2012; Nade et al., 2015; Narayanan et al., 2017). The EPBs obtained in images of ASI are usually not linear; it shows complex structures pertaining to its morphology. This complex configuration of the EPBs was found to be dominant at off-equatorial pole ward side of the ASI images. However, to understand the EPBs completely, it is very important to investigate their structural morphology and evolution.

Sahai et al., (2006) reported that the western wall is the most unstable side of EPBs which results into bifurcation. First time, the phenomenon like bifurcation of EPBs was observed from ground based OI 630.0 nm imaging at Ascension Island (Mendillo and Tyler, 1983). Based on numerical simulations McDonald et al. (1981) and Zalesak et al. (1982) showed that bifurcation occur when the ratio of E-region Pedersen conductivity to F-region conductivity becomes less than 10 inside and outside of EPBs. Moreover, electric field and upward motion of charged particles inside the EPBs may be responsible for increasing east-west dimension of EPBs and thus bifurcation might occur in the EPBs (Huang and Kelley, 1996; Yokoyama et al., 2014). Generally, EPB grows non-linearly after the post sunset period; the topside of EPB has a steep upward density gradient which makes it so unstable that the bifurcation can easily occur (Yokoyama et al., 2014). Huba and Joyce (2007) observed that the bifurcation of EPBs occurred below the F region peak altitude over low latitude region. Sometimes the bifurcation appeared on the eastern wall of EPB which was tilted towards west with corresponding apex height was typically above 500 km (Zalesak et al., 1982). Huang and Kelley (1996) suggest that some EPBs could eventually bifurcate if their east-west elongation has significantly large in dimension up to few hundred kilometers.

Huang et al. (2012) observed plasma depletions spanning over several hundred kilometers in longitude by C/NOFS during solar minimum. They interpreted that the broad depletions are formed due to merging of multiple EPBs. Further, Huba et al. (2015) studied merging of EPBs using SAMI3 model and found that the EPBs merge through the electrostatic reconnection in the ionosphere. They suggest that merging occurs when the electrostatic potential linked with one EPB can connect with adjacent EPB in such way that the low density plasma channels of the EPBs merge together. Further, they reported that there is indeed a strong unevenness in neighboring EPB such that their $E \times B$ drifts are oppositely directed. Narayanan et al. (2016a) reported evidences of EPBs merging using optical imaging observations carried out from low latitude Indian region. They suggested three mechanisms for merging of EPBs. First, the merging occurs when one of the EPBs tilts and meets the channel of neighboring EPB. Second, secondary structures developed in EPBs may merge within the adjacent EPB. Third, EPB on the eastern side slows down in its drift and upcoming EPB from west merges with it.

Laakso et al. (1994) using San Marco D satellite measurements showed that, the usual eastward electric field becomes westward just prior to mid-night. As a result of this, the plasma inside the depleted EPBs over the magnetic equator at an altitude of ~400 km or less may experience the downward motion. However, at the higher altitudes, in the same EPB the plasma motion remains upward. This opposite drift at different altitudes inside the same EPB over the equator may led to detachment of upper part of the EPB from the lower one. Sahai et al. (2006) reported that the detachment of EPBs structures were possibly associated with the development of non-homogenous vertical plasma drift due to non-homogeneous eastward electric field. This further creates the zonal plasma drift gradient over the low latitude region which makes EPBs to detach into different parts. Recently, Chian et al. (2018) studied spatiotemporal dynamics of ionospheric intermittent turbulence using non-linearity in optical images recorded by multi-spectral all-sky imager in the South Atlantic Magnetic Anomaly region. They showed that, the degree of non-Gaussianity, intermittency and multifractality is stronger in the North-South direction, confirming the anisotropic nature of the interchange instability.

The present study focuses on the interesting observations of bifurcation, merging and detachments of EPBs using all sky image data of nightglow OI 630.0 nm emission.

2. Instrumentation, data collection and analysis

The observations of nightglow OI 630.0 nm emission have been carried out using ASI since October 2010 from Kolhapur. The instrument is still under operation. We have analyzed ASI data of OI 630.0 nm emission from October 2010 to December 2015 for the present study. The multi-spectral (OH, OI 630.0 and OI 577.7 nm emissions) ASI has been installed at Shivaji University Campus, Kolhapur under the scientific collaborative program between Shivaji University, Kolhapur (S.U.K.) and Indian Institute of Geomagnetism (I.I.G.), Navi Mumbai, India to study the dynamics of ionospheric irregularities. A high resolution (1024×1024 pixels) Charge Coupled Device (CCD) based ASI has 140° operating field of view (FOV) (refer Fig. 1) and covers an approximate horizontal distance of about ~1220 km in diameter at an altitude of 250 km (Sharma et al., 2014, 2018). The details of ASI can be found

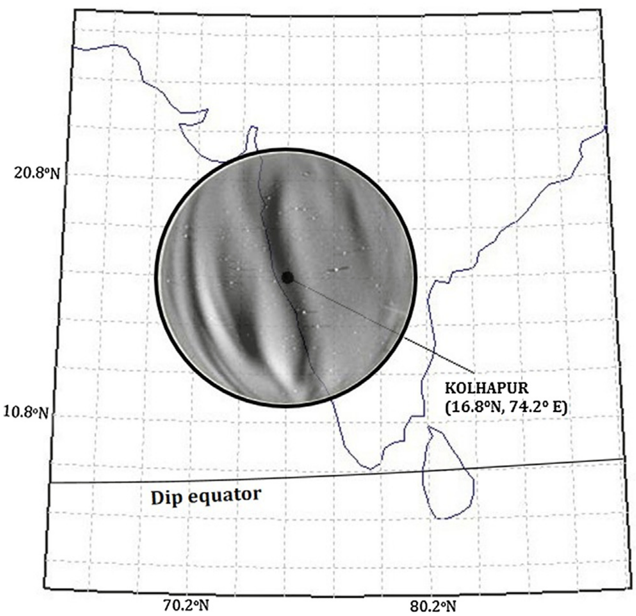

Fig. 1. Schematic of the field of view of ASI as 140° from Kolhapur location which covers horizontal distance of ~1220 km.

elsewhere (Ghodpage et al., 2014, 2018). The OI 630.0 nm images on selected nights have been processed using averaging method described by Sharma et al. (2014). The processed images clearly shows the structure of EPBs as dark bands, which we have considered for further analysis to study the characteristics of EPBs. Also the equidistance projection of ASI images are made assuming an altitude of 250 km altitude for the field of view ~140° (Narayanan et al., 2009). In present study, we have used east-west scanning method which is described by Pimenta et al. (2001) to calculate the drifts of EPBs. In our method, we have scanned ASI images by east-west direction with 20 pixel strip. Each column of 20 pixels in this strip is averaged to plot intensity curves to avoid random fluctuations in the intensities of OI 630.0 nm emission following Narayanan et al. (2017). The intensity data used here are detrended and smoothed by 50 point running average to further reveal EPB features properly. The plots show the longitudinal offset of EPBs during the course of night. This shifting of EPBs is used to calculate their drift. The east-west cross sections are taken wherever needed. Further, we have measured tilt angles of EPBs wherever necessary. For this, we take a line along the center of an EPB for which the tilt angle is to be determined. The angle between this line with the abscissa will give the tilt angle of the EPB in degree from geographic north. Because equidistance images are made such that top of the images correspond to the geographic north. This tilt angle is subtracted from the declination of Kolhapur (~0.54°W) to get the angle from geomagnetic north.

In the all-sky imager data, we have identified some nights showing interesting features of EPBs such as bifurcation, merging and detachment of EPBs. All these nights discussed here are geomagnetically quiet. Herein we have reported eight events recorded on different nights as below. Bifurcation on 20–21 January 2012 and 13–14 December 2012, merging events on 08–09 March 2011 and 16–17 December 2012, complex evolution features involving merging on 06–07 March 2013 and detachment of EPBs observations on 31 March-01 April 2011, 19–20 January 2012 and 25–26 April 2015.

3. Results and discussions

3.1. Bifurcation characteristics of EPBs

On occasions, the depleted density regions of EPBs show branched structures on sides of their main stem. Such branched features are termed as bifurcated EPBs. Fig. 2 shows the bifurcation observation on the night of 20–21 January 2012. Here initially at 17:22 UT, a dark structure is seen entering from the west into the field of view of ASI. Initially, we see that it is a single EPB, but on later time, one can notice that the top structure of the EPB has two branches, namely b1 (east one) and b2 (west one) as shown at 18:39 UT. The bottom of the EPB can be termed as its trunk t1. As time progress, the top branched structures (b1 and b2) exhibits more separation from each other. Here, the eastern part i.e. b1 is an evolving feature. To analyze these changes in detail, we have taken E-W cross sections at the top and bottom portions of whole EPB as shown in Fig. 2. The red line indicates the E-W scan through b1 and b2 (branched structures). The yellow line indicates the E-W scan through trunk t1 of EPB. Using the longitudinal offset in EPBs position in the scanned data, we have calculated the zonal drifts of the bottom portion (i.e. trunk) of EPB as well as the distance between the b1 and b2. The measured values of zonal drifts of the bottom trunk t1, distance between b1 and b2 and the tilt angle are plotted against the time as shown in Fig. 3. The drift of the trunk t1 was between ~40 m/s and ~60 m/s. The eastern branch b1 has evolving nature and this makes the bifurcation and the distance between the b1 and b2 is also increased during the course of time as can be seen in the top portion of Fig. 3. Since b1 is an evolving feature, it is inappropriate to discuss its drift which may be affected due to the evolving structure. The tilt angle of the whole EPB is calculated as shown in Fig. 2 (see 17:43 UT) by green arrows. The vertical green arrow is parallel to geographic north and west tilted arrow is drawn through the linear portion of the EPB. This gives the tilt angle of that EPB in degree from geographic north. Please refer Section 2 for measurement of tilt angle of EPB. It is also important here to note that throughout this bifurcation the tilt of the whole EPB found to be increased during the course of time as can be seen in the middle panel of Fig. 3. After bifurcation of EPB, the bifurcated branches become diffuse at later time. In Fig. 2, the branched structures b1 and b2 is diminished (diffused) as can be seen in the bottom row of ASI images. We also find only some of the EPBs show bifurcated features.

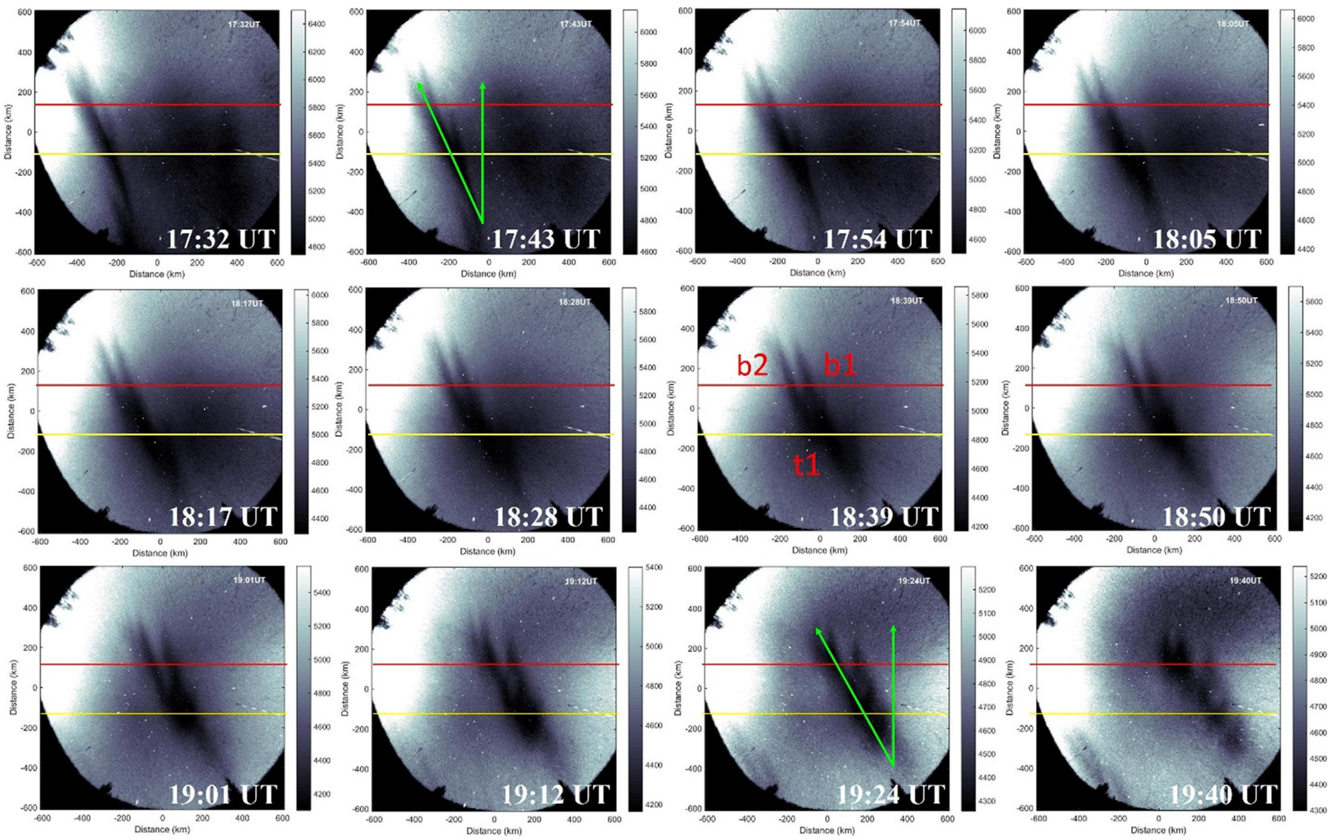

Fig. 2. OI 630.0 nm images from Kolhapur on 20–21 January 2012. Top and right corresponds to the north and the east, respectively.

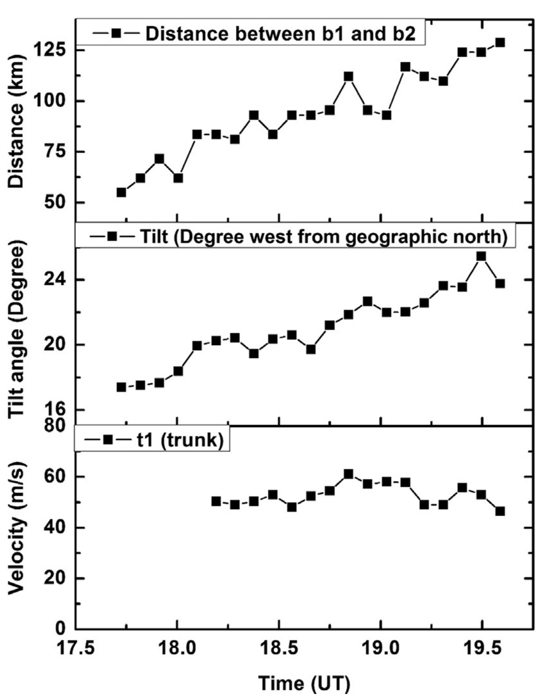

Fig. 3. Zonal drift of b1, b2 and b3, tilt angle and interdepletion distance between b1 and b2 against local time for the night of 20–21 January 2012.

Another bifurcation phenomenon is observed on the night of 13–14 December 2012. In this case, initially four EPBs namely b1, b2, b3 and b4 (numbered from east to west) entered into the FOV as shown in Fig. 4. As time progress, the secondary features are generated at the top of b3 and b4 as shown by green arrows at 19:33 UT. Meanwhile, b2 weakens and disappears with time. Such disappearance of EPB is earlier noticed by Shiokawa et al. (2015). The secondary features generated at the top of b3 and b4 evolves with time and looks similar to bifurcated arms. It is important to note here that, the secondary features appeared as bifurcating arms from its corresponding EPBs starts moving eastward as well as southward. Meaning, the bifurcated structures stops its growth and starts shrinking towards the equator (Please refer to EPBs shown at 20:24 UT by green arrows in Fig. 4). Shrinking of the EPBs is a new finding made recently by Narayanan et al. (2016b). They suggest that, when polarization electric field inside EPBs decays, it will stop growing and might decay before sunrise. Further, the present case is different than that of reported recently by Xiong et al. (2018). They observed bifurcation of EPBs on 24th September 2014 using all-sky imager at Fuke, south of China. They found the bifurcation of EPBs at higher as well as lower latitude-parts, with EPBs having

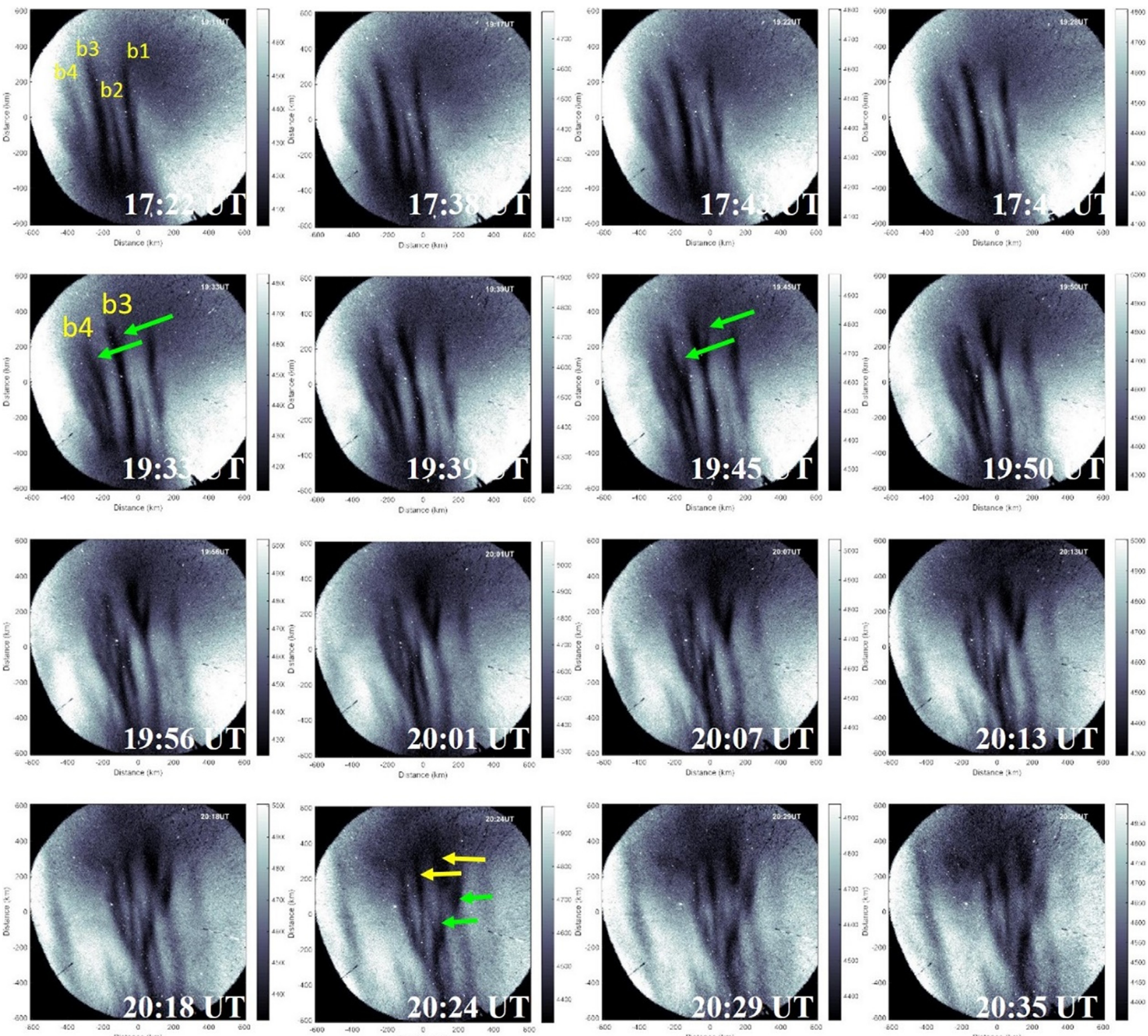

Fig. 4. OI 630.0 nm images from Kolhapur on 13–14 December 2012. Top and right corresponds to the north and the east, respectively.

very thinner structures about 25–30 km in width. Moreover, these slender bifurcating structures were growing to higher latitude parts unlike in present case where they are shrinking towards the equator. Further, they suggested that, the density distribution inside the EPBs were very turbulent in nature during this bifurcation. In the previous as well as in the present case, the bifurcation occurred towards pole ward side of FOV (or at the top portions of EPBs) which corresponds to greater apex height.

3.2. Merging characteristics of EPBs

The interesting phenomenon of merging of EPBs is observed on the night of 08–09 March 2011 around pre midnight period. Fig. 5 shows the sequence of OI 630 nm airglow images recorded on this night. Initially three EPBs are found in the FOV namely b1, b2 and b3 which enter from west. As time progress, b1 disappeared. The top of b2 has two branched structures shown by red arrows at 16:18 UT which are initially tilted towards west. The branching is result of bifurcation. The tilt angle of this top structure becomes almost zero at 16:47 UT and with further time, exhibits some eastward tilt. Also the top portion of b3 changes as part of its evolution and finally b3 gets merged into adjacent b2. Here, the upcoming b3 has bulge at its top which merges with the b2. Further, it is noted that the b3 has reached to lesser apex altitude than b2 while it was merging. This is similar to one of the mechanisms discussed in Narayanan et al. (2016a). To understand this scenario, two E-W cross sections of ASI

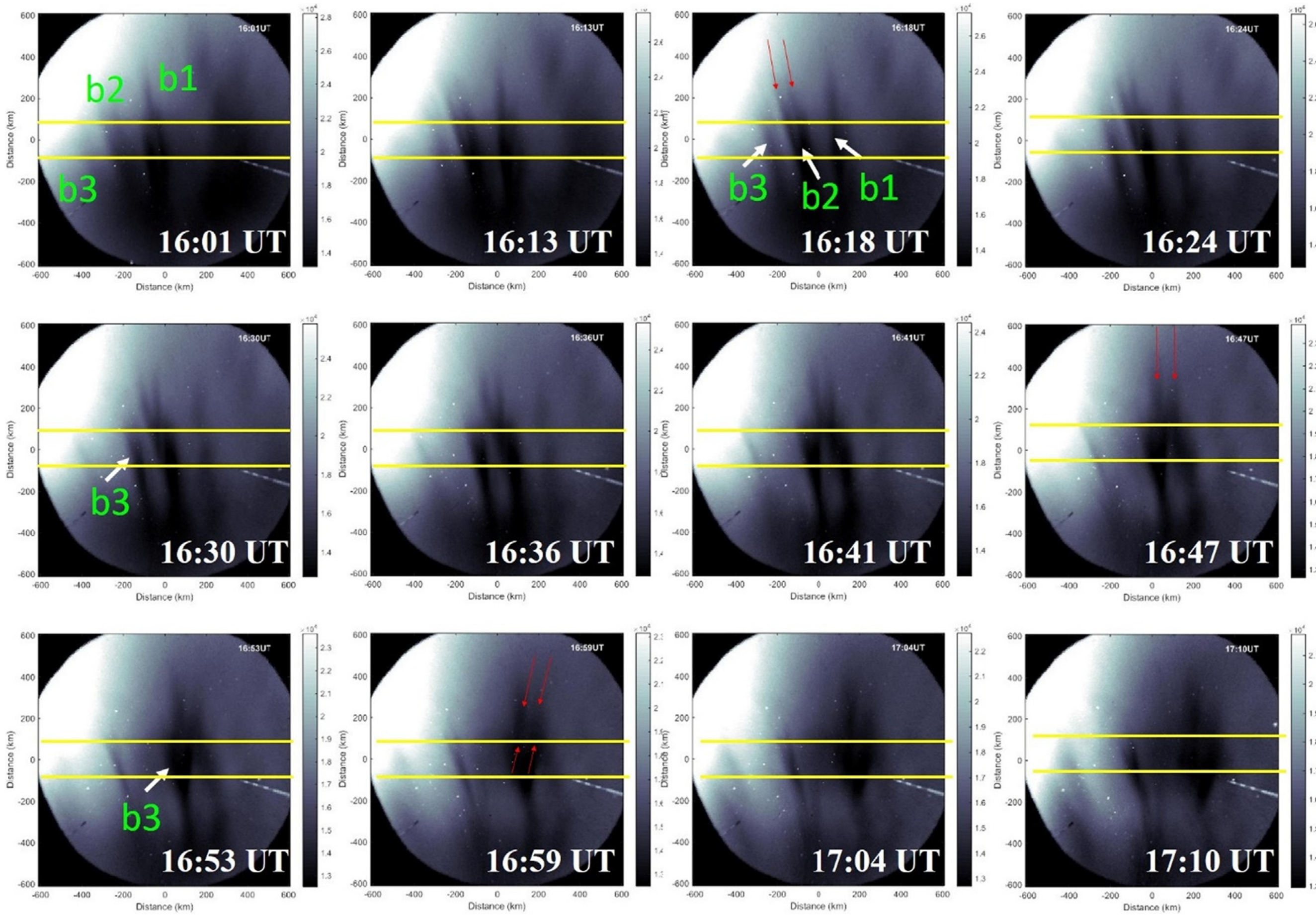

Fig. 5. OI 630.0 nm images from Kolhapur on 08–09 March 2011. Top and right corresponds to the north and the east, respectively.

images (one is at top +100 km and other is at bottom −100 km from zenith shown by yellow horizontal arrows in Fig. 5) are taken. The extracted intensity plots are shown in Fig. 6. In the left panel which corresponds to the top portion of the EPBs, it is seen that b3 moves towards the adjacent b2 and finally merges with it at 16:47 UT shown by pink horizontal arrow. While in the right panel which corresponds to the bottom portion, b3 moves continuously towards east without merging with b2 which also drifts to the east. In left panel of Fig. 6, b3 merges in b2 at 16:47 UT due to tilt reversal at top portions of EPB. While the right panel shows b3 and b2 separately as there is no significant tilt changes in the bottom part of the same EPBs. So no merging is observed at the bottom part. And hence b2 and b3 (blue and red respectively) moves eastward separately without merging. Further, b1 and b2 disappears as time progress. From this case, we infer that the merging occurs at the top side of EPBs than that of bottom side. In our case, the merging occurred due to the tilt changes as well as the non-linear evolution at the top portions of EPBs. These are similar to the mechanisms identified in Narayanan et al. (2016a).

Another case of merging is observed on the night of 16–17 December 2012. In Fig. 7, initially we highlight b1 and b2 which entered from west. It may be noted that these EPBs are post-mid night EPBs. They are almost linear in shape along the magnetic field lines. When time progress, b3 rises into the FOV and it later show some structures forming at its western wall. As far as b2 is concerned, its top portion shows bulge of depletion and its middle and bottom part has relatively thinner width. As time progress, b3 grows and merges in the top portion of adjacent b2 as shown in Fig. 7 at 22:04 UT. Further, it is noted that, the b2 into which b3 merges has larger apex altitude than b3. This merging is caused due to the post-mid night growth of EPB. Later on, b1 and b2 are weakened that they are difficult to recognize in the images. Further, all the structures formed on b3′s west arm tends to diffuse and forms a single EPB as can be observed in the final few ASI images. Also, after merging, b3 exhibits a slight eastward tilt. With time, the width of the b3 is noticed to increase and shortly after merging the tilt becomes eastward. The increased scale size (width) might be one of the reason to the eastward tilt after merging. Further, the finer variations in the latitudinal gradient in zonal neutral wind along the meridian (corresponding to altitudinal shear) also might be responsible for eastward tilt of this structure.

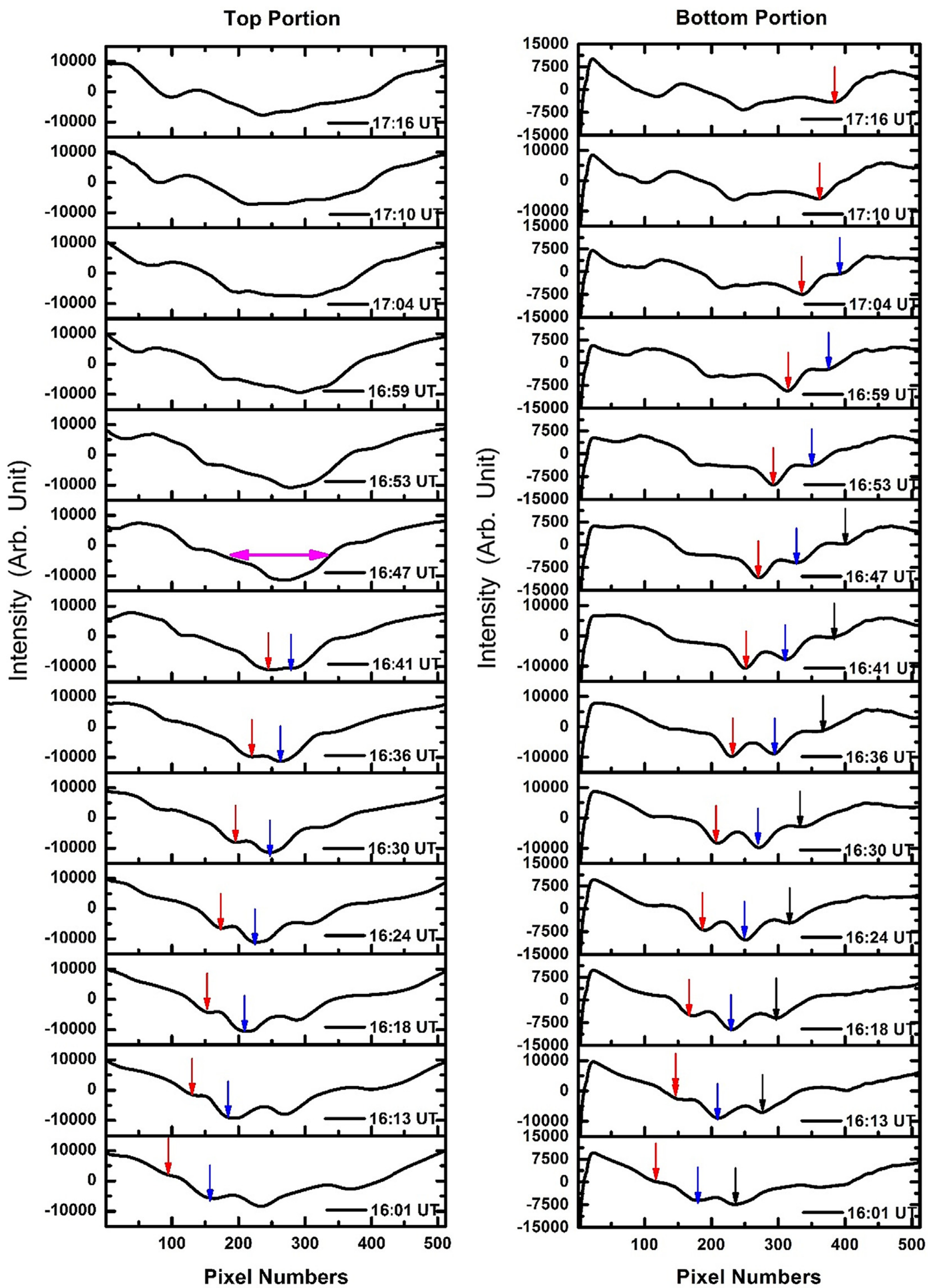

Fig. 6. East-west scan of all sky images recorded on 08–09 March 2011 showing merging of b2 into b3. The b1, b2 and b3 are shown by black, blue and red arrows respectively. (For interpretation of the references to color in this figure legend, the reader is referred to the web version of this article.)

We observed another interesting yet complex evolving feature of EPBs on the night of 06–07 March 2013. In Fig. 8, we highlighted b1 initially. Later on we observed other two arms as b2 and b3. Please note that all these arms b1, b2 and b3 appear to form on a single EPB. While all these branches has single base (trunk), the merging is occurring on the top side of the EPB between the branches. After 17:30 UT, top portion of b2 tends towards east, i.e.

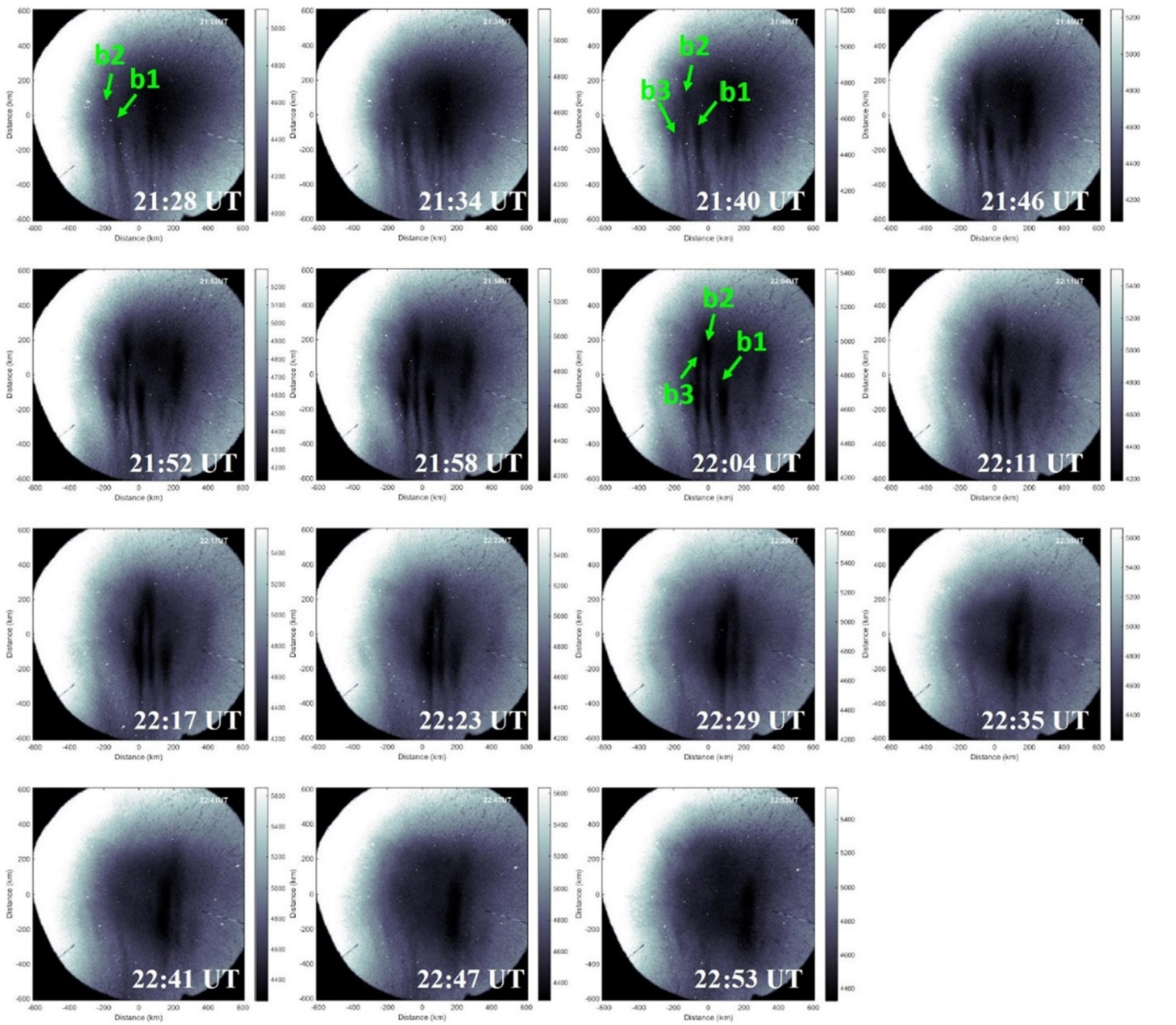

Fig. 7. OI 630.0 nm images from Kolhapur on 16–17 December 2012. Top and right corresponds to the north and the east, respectively.

towards b1 and later on, it merges with b1 from 17:46 UT onwards. Therefore the b2 changes its tilt from westward to eastward and meets the channel of adjacent arm b1. Further, the tilt angle of this whole EPB gets reversed to eastward after the merging as can be seen in Fig. 8 (shown by inclined green line before merging and red line after merging). The b3 also gets tilted towards east. To study this event more clearly, we have calculated the zonal drifts of top (horizontal green line) and bottom (horizontal yellow line) portions of this EPB as shown in Fig. 9. It is found that the top portion is moving comparatively faster than that of bottom portion after 17:00 UT. Also, when top portion is moving faster, the bottom portion slows down in its drift velocity up to 17:45 UT. This discrepancy in drift makes the EPBs slightly tilted to the east after 17:45 UT. The latitudinal/altitudinal gradient in drift causes eastward tilt of EPBs as shown by red arrow in Fig. 8. Further, we have measured the tilt angles of this whole EPB structure and plotted against time as shown in bottom panel of Fig. 9. The large drift of top portion of this EPB is responsible for eastward tilt which can be observed as negative tilt angle values. In this case, the merging has occurred due to the tilt reversal. This type of merging is also explained by Narayanan et al. (2016a) in which they explained that merging occurs when one EPB tilts and meets the channel of adjacent EPB. However, in this case similar merging happens between branches of a larger size EPB.

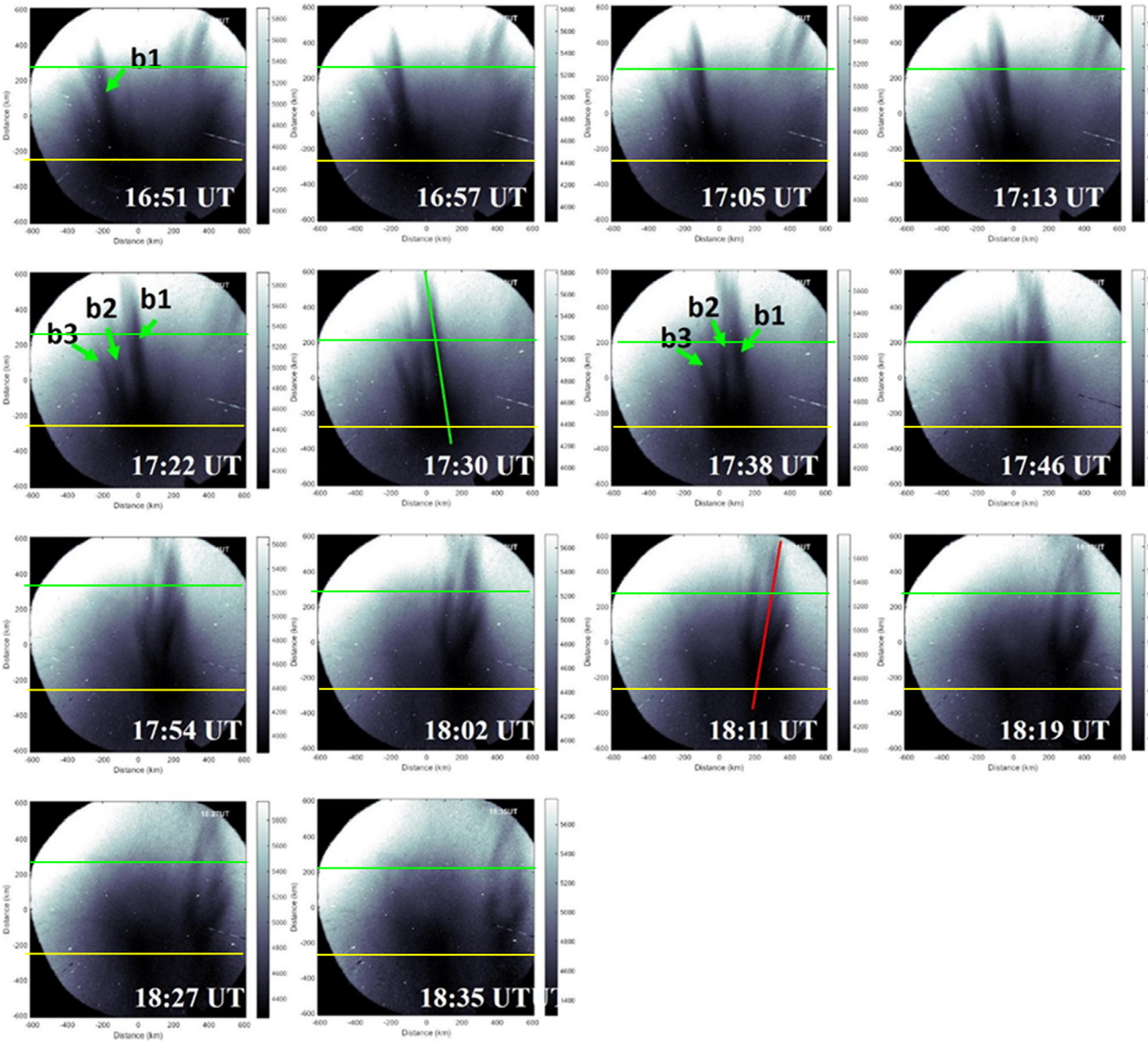

Fig. 8. OI 630.0 nm images from Kolhapur on 06–07 March 2013. Top and right corresponds to the north and the east, respectively.

3.3. Detachment characteristics of EPBs

On occasions, EPBs are seen to separate as a part from the main stem, which is referred to as detachment of EPB structures. Such features are observed on the night of 31 March-01 April 2011 from Kolhapur. In Fig. 10, initially a single EPB enters from west into the FOV where its depletion level is low. As time progress, the top portion of this EPB shows bifurcated structures, namely b1 and b2 shown at 23:14 UT. The west arm is shown as b2 and east arm is shown as b1. These are the post mid-night EPBs. We can see that, from 23:03 UT, the enhancement (E1) in the bifurcation region is moving downward, splitting the EPB. The detached part on the right side i.e. b2 moves in southward (equator ward) direction while b1 remains unchanged. Unfortunately we don't have the recording of ASI 630.0 nm images further towards the dawn period. The east-west keograms at ±50 km from zenith (or center of image) are shown in Fig. 11 which also reveals that the enhancement region (E1) splits the EPBs into two parts. In this case, there is equator ward motion of detached part apart from the usual eastward motion. This phenomenon called shrinking of EPBs has been studied in some detail by Narayanan et al. (2016b) from low latitude Indian region. They found the decrease in latitudinal extent of the EPBs corresponding to a reduction in their apex altitudes over the dip equator. In present case, initially EPB is seen to drift towards east with no equator

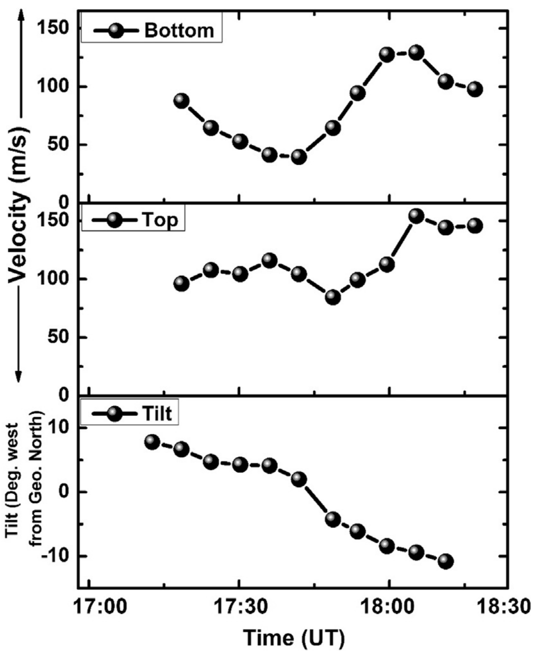

Fig. 9. Zonal drift velocities of top and bottom portions of the EPBs for the night of 06–07 March 2013.

ward motion. But when one of its bifurcated arm detaches, that detached eastern arm moves equator ward or shrinks.

Another detachment feature is observed on the night of 19–20 January 2012. In Fig. 12, a single EPB shown in the oval entered from the west which consists of bifurcated arms. We named them as b1, b2 and b3. The b1 starts detaching from b2 at 16:14 UT. Please note that, b1 and b2 comprise the whole east arm of this EPB. The pole-ward extension of b1 indicates that it is in development phase. At 16:32 UT, we can see that the b1 gets separated from b2. As time progress, b2 becomes too weak to be detected. The b1 also becomes weaker but still detectable. And at the bottom panel, only b3 remains. We have taken cross section of images around +200 km for top and around −100 km for bottom along y axis as shown by red and yellow color lines respectively. We have measured drifts of b1 (top) and b3 (bottom) separately as shown in Fig. 13. Note that initially bottom portion was moving relatively slower. With time the drift in the lower portion increased sharply, while the top portion was of nearly same drift though. At the same time, the top portion not only pinched but its tilt also changed. This event shows that

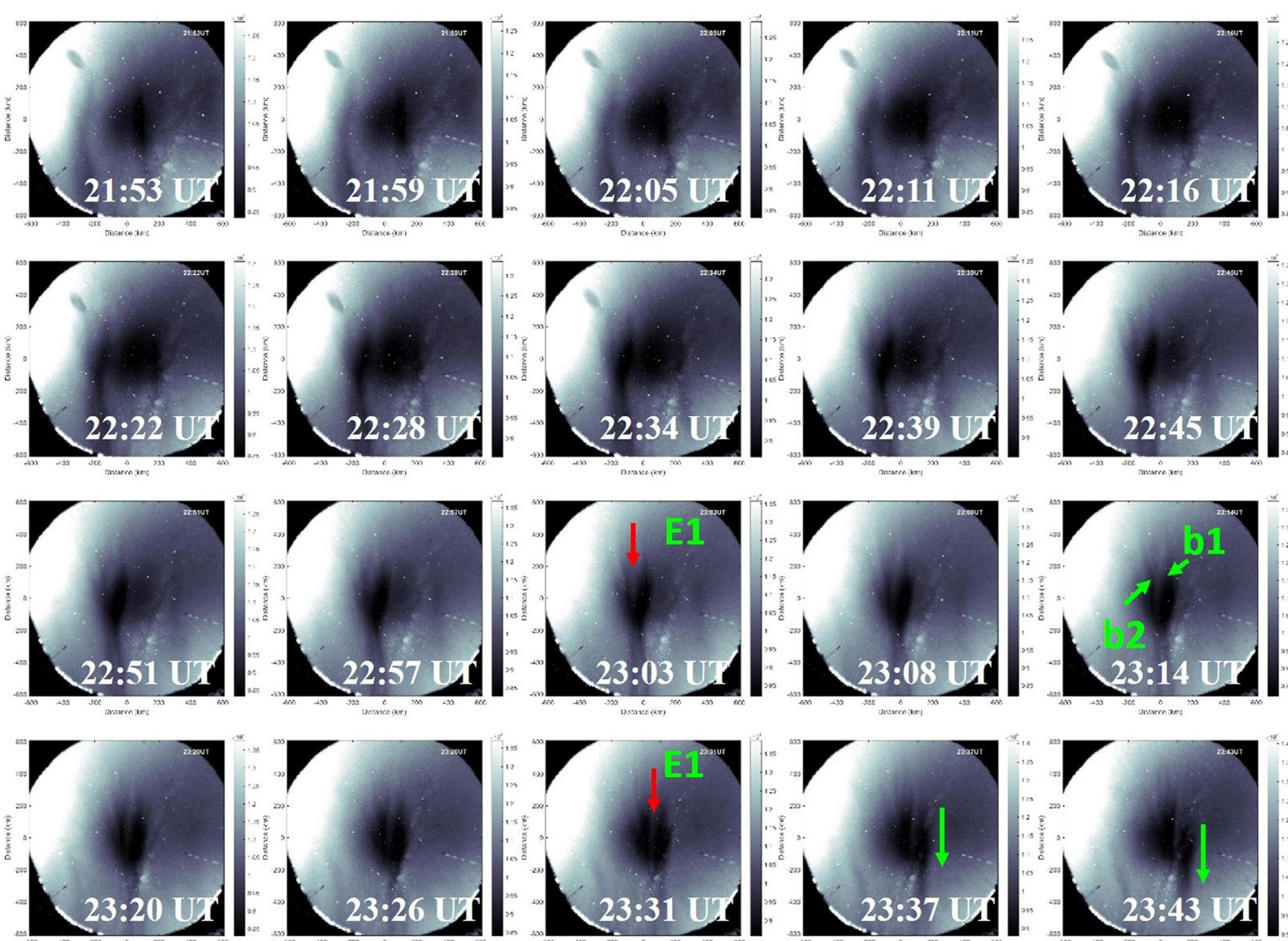

Fig. 10. OI 630.0 nm images from Kolhapur on 31 March-01 April 2011. Top and right corresponds to the north and the east, respectively.

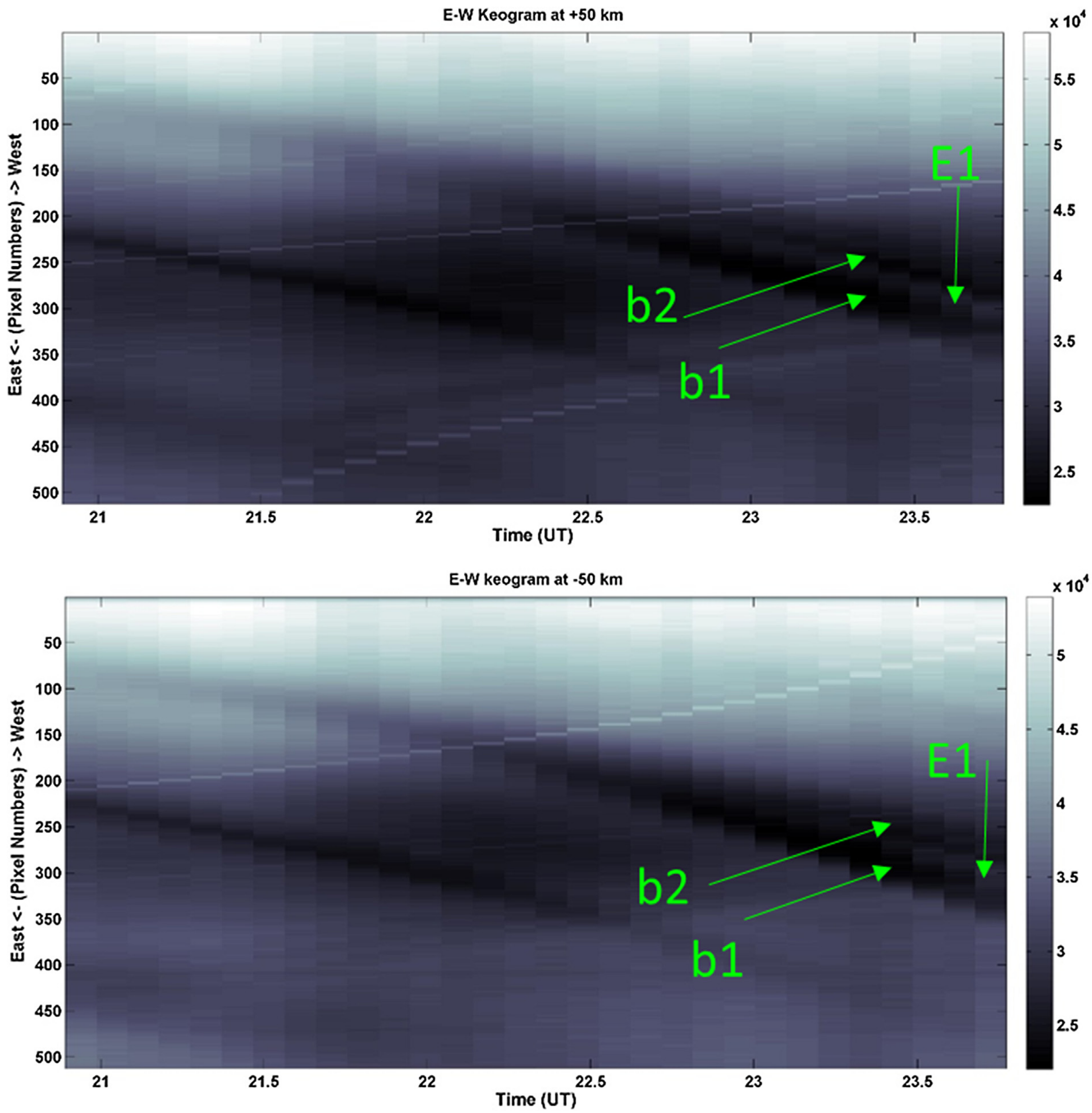

Fig. 11. The east-west keograms taken at ±50 km from zenith (or center of image) for the night of 31 March-01 April 2011.

the zonal drift corresponding to different portion of the EPB is also different when detachment occurs. Laakso et al. (1994) attributed pinching to the different vertical drifts. Initially the top portion was tilted towards the west. Around 16:50 UT its tilt is almost zero and it becomes straight along the north-south direction in the middle. With time, it is further leaning towards east.

In Fig. 14, we present detachment of EPBs observed on the night of 25–26 April 2015. Initially the EPB shown as b1 is moving towards east. As time progress we can see that the top portion of this EPB is moving very slowly and the bottom portion is moving faster which eventually gets detached from its top portion around 21:18 UT. After detachment, the bottom portion shrink and disappear afterwards. This detachment occurred due to unequal drifts of EPBs top and bottom portions similar to previous case. The east-west cross section is taken at top (red +300 km from zenith) and at bottom (yellow −145 km from zenith). The bottom portion moved faster than top portion which causes the detachment of bottom portion from the upper one. It is clearly seen in the drift measurement shown in Fig. 15 that, the top portion is drifting comparatively slower than bottom portion. Further, note that the change in their drifts were opposite to each other (colored patch shown in Fig. 15) where the separation during the detachment is larger.

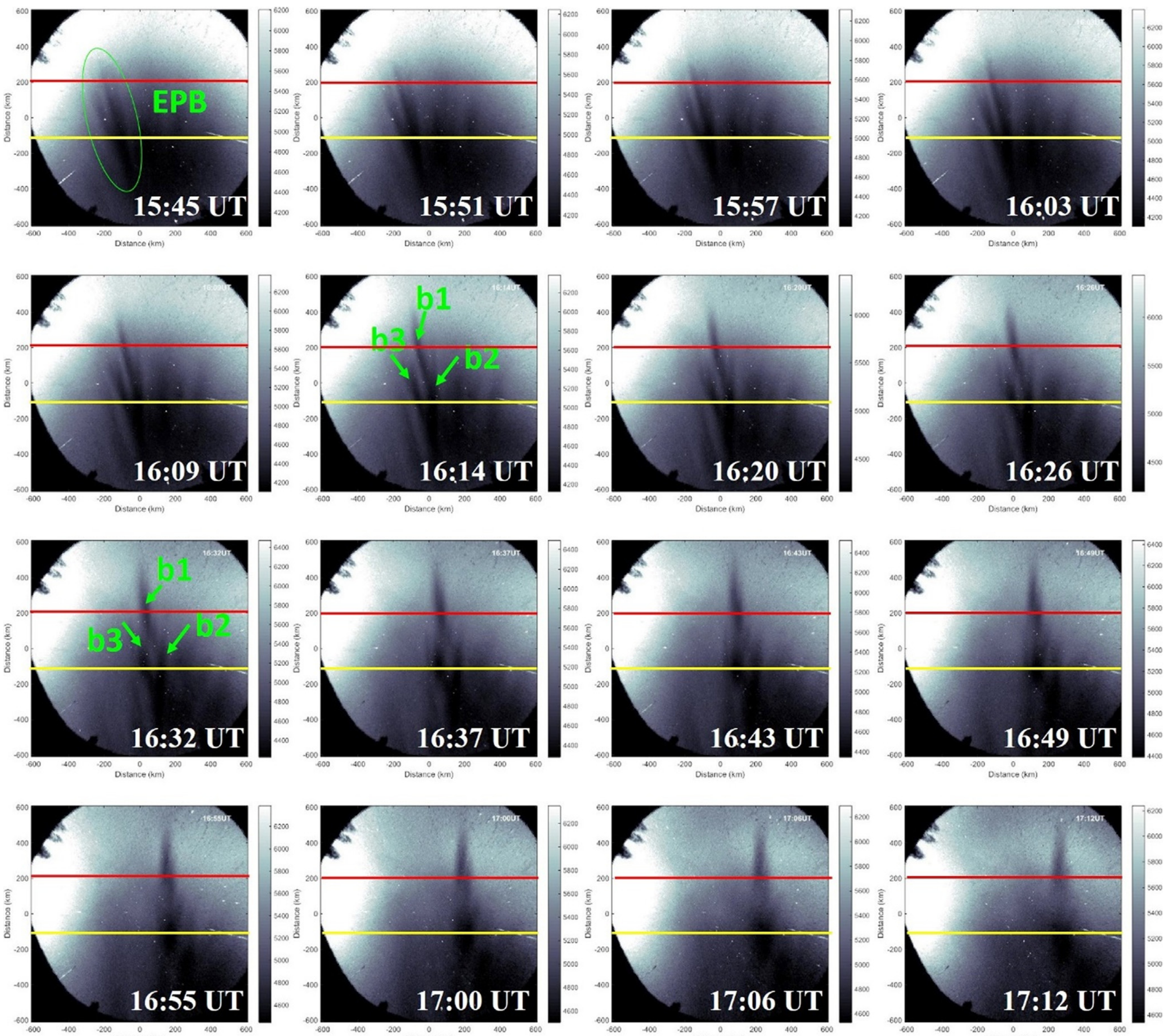

Fig. 12. OI 630.0 nm images from Kolhapur on 19–20 January 2012. Top and right corresponds to the north and the east, respectively.

4. Conclusions

Based on observations of OI 630.0 nm nightglow emission using ASI from low latitude station Kolhapur, we have found some interesting features related to evolution of EPBs which are listed below.

1. The evolution of secondary features on the eastern side of the EPBs are observed on the night of 13–14 December 2012. These secondary features seems like bifurcating structure on the eastern wall of EPBs. Probably, the eastern wall of the EPBs are most unstable where the bifurcation can easily occur.
2. We observed that, the merging in EPBs occurs when one EPB tilts and meets the channel of adjacent EPB. The change in tilt is probably due to the faster drifts of top than that of bottom parts of the EPBs. The latitudinal gradient in zonal neutral wind might have contributed to change in drifts causing tilt variations. Also, the merging is observed only in the top portion and not in bottom portion of EPBs in this work. Nevertheless, the observed merging appear to support the earlier mechanisms proposed by Narayanan et al. (2016a).
3. The detachment in EPBs appear to occur due to the large shears in zonal drift velocity with time between top and bottom portions.
4. We also note that EPBs shrink on occasions.

To conclude, morphology of EPBs and its evolution has been studied by many researchers. In this work, we report few features which agree to the previous findings and some are new warranting further study. These kinds of studies are important to improve the understanding of evolution mechanisms of EPBs.

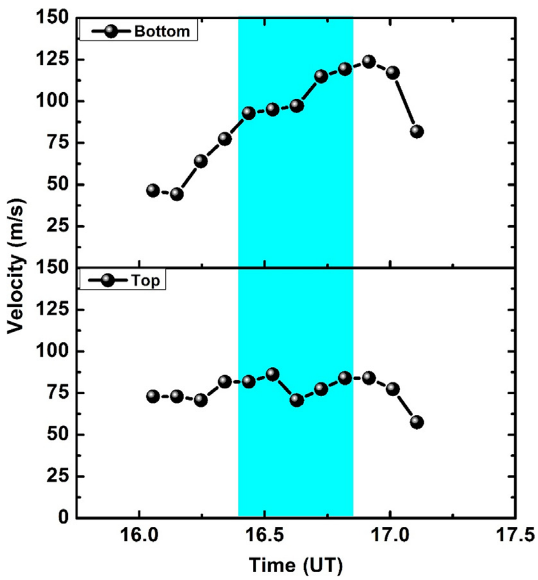

Fig. 13. The zonal drifts of top and bottom portions of the EPB for the night of 19–20 January 2012.

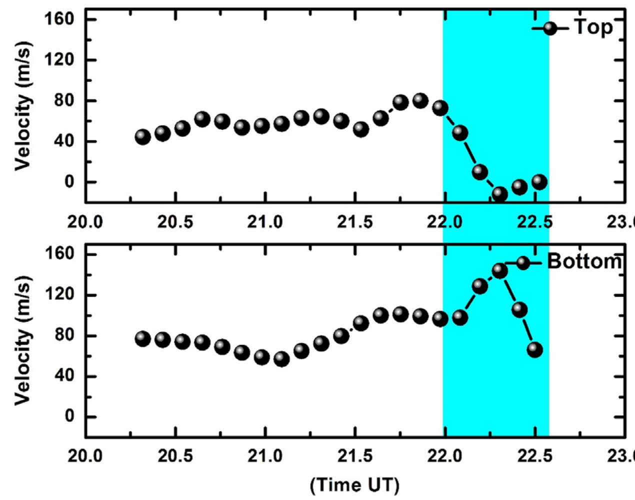

Fig. 15. The zonal drift of b1 and b2 against local time for the night of 25–26 April 2015.

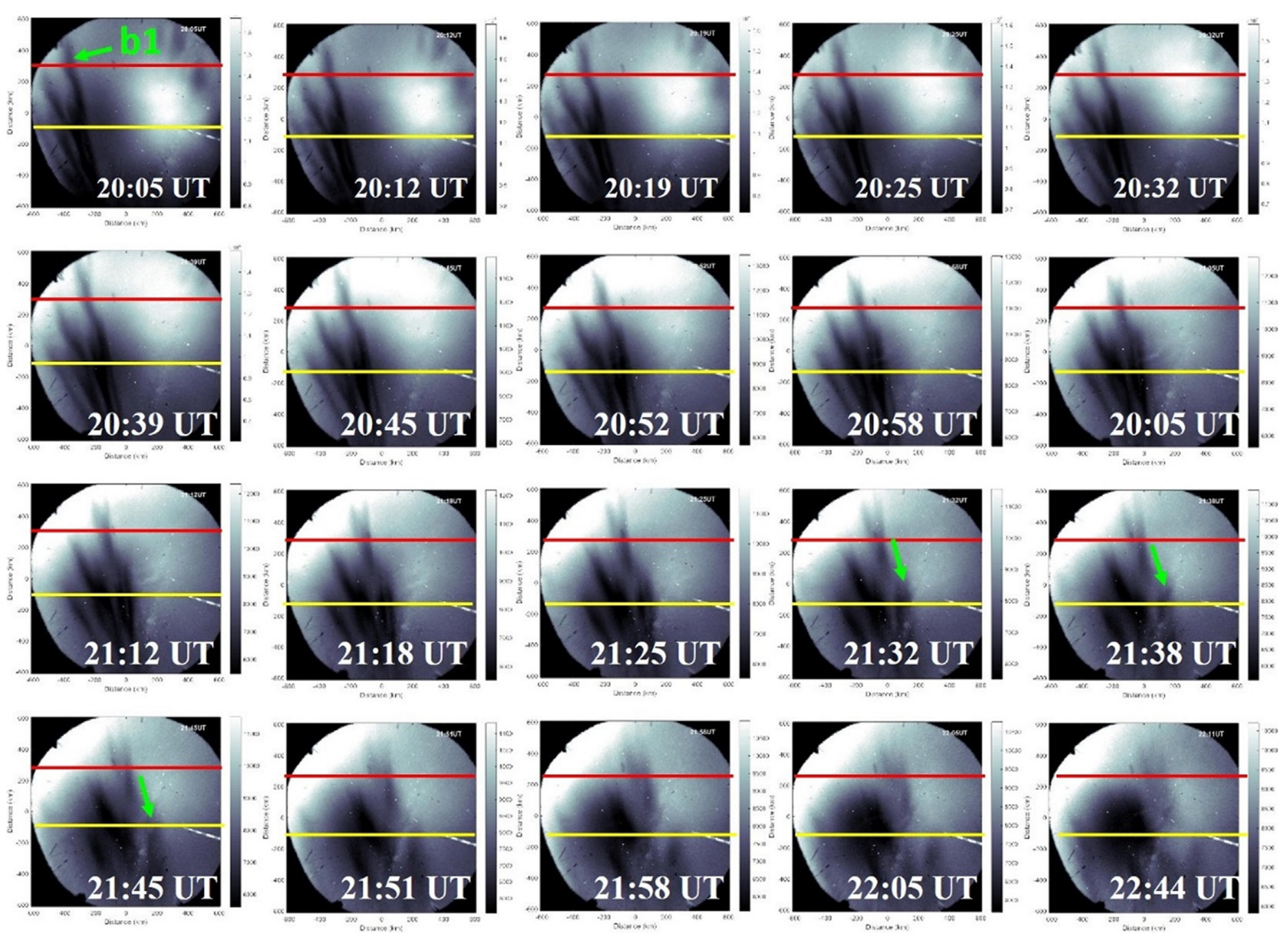

Fig. 14. OI 630.0 nm images from Kolhapur on 25–26 April 2015. Top and right corresponds to the north and the east, respectively.

Acknowledgement

The observations of night airglow using all-sky imager is carried out from Kolhapur under the scientific collaboration program between Indian Institute of Geomagnetism (I.I.G.), Navi Mumbai, India and Shivaji University, Kolhapur (S.U.K.). We are thankful to IIG, Navi Mumbai for providing the OI 630.0 nm image data. The data used in this work can be accessed by contacting S. Gurubaran (gurubara@iigs.iigm.res.in) from IIG. This work is mainly supported by Basic Scientific Research (BSR) Fellowship of University Grants Commission, New Delhi, India, awarded to O. B. Gurav (F.25-1/2014-15(BSR)/7-167/2009/BSR, October 2015). V. L. Narayanan thanks Department of Science and Technology, India for support through INSPIRE Faculty grant number DST/INSPIRE/04/2014/001636.

References

Chian, A.C., Abalde, J.R., Miranda, R.A., Borotto, F.A., Hysell, D.L., Erico, L.R., David, R., 2018. Multi-spectral optical imaging of the spatiotemporal dynamics of ionospheric intermittent turbulence. Sci. Rep. 8 (1), 1–15. https://doi.org/10.1038/s41598-018-28780-5.

Dao, T., Otsuka, Y., Shiokawa, K., Ram, S.T., Yamamoto, M., 2016. Altitude development of postmidnight F region field-aligned irregularities observed using Equatorial Atmosphere Radar in Indonesia. Geophys. Res. Lett. 43 (3), 1015–1022. https://doi.org/10.1002/2015GL067432.

England, S.L., Immel, T.J., 2012. An empirical model of the drift velocity of equatorial plasma depletions. J. Geophys. Res. Space Phys. 117 (12), 1–9. https://doi.org/10.1029/2012JA018091.

Ghodpage, R.N., Taori, A., Patil, P.T., Gurubaran, S., Sripathi, S., Banola, S., Sharma, A.K., 2014. Simultaneous optical measurements of equatorial plasma bubble (EPB) from Kolhapur (16.81N, 74.21E) and Gadanki (13.51N, 79.21E). J. Atmos. Sol. Terr. Phys. 1–10. https://doi.org/10.1016/j.jastp.2014.05.008.

Ghodpage, R.N., Patil, P.T., Gurav, O.B., Gurubaran, S., Sharma, A.K., March 2018. Ionospheric response to major storm of 17th March 2015 using multi-instrument data over low latitude station Kolhapur. Adv. Space Res. 63 (3), 624–637. https://doi.org/10.1016/j.asr.2018.05.003.

Gurav, O.B., Sharma, A.K., Ghodpage, R.N., Nade, D.P., Chavan, G.A., 2018. Zonal drift velocity of Equatorial Plasma Bubbles during ascending phase of 24th solar cycle using All Sky Imager over Kolhapur, India, https://www.doi.org/10.1029/2018JA025810.

Huang, C.S., Kelley, M.C., 1996. Nonlinear evolution of equatorial spread F 2. Gravity wave seeding of Rayleigh-Taylor instability. J. Geophys. Res. 101, 293–302.

Huang, C., Retterer, J.M., La Beaujardiere, O.D., Roddy, P.A., Hunton, D.E., Ballenthin, J.O., Pfaff, R.F., 2012. Observations and simulations of formation of broad plasma depletions through merging process. J. Geophys. Res. Space Phys. 117, 1–11. https://doi.org/10.1029/2011JA017084.

Huba, J.D., Joyce, G., 2007. Equatorial spread F modeling: multiple bifurcated structures, secondary instabilities, large density “bite-outs”, and supersonic flows. Geophys. Res. Lett. 34 (7), 1–5. https://doi.org/10.1029/2006GL028519.

Huba, J.D., Wu, T., Makela, J.J., 2015. Electrostatic reconnection in the ionosphere. Geophys. Res. Lett. 42 (6), 1626–1631. https://doi.org/10.1002/2015GL063187.

Immel, T.J., Frey, H.U., Mende, S.B., Sagawa, E., 2004. Global observations of the zonal drift speed of equatorial ionospheric plasma bubbles. Ann. Geophys. 22 (9), 3099–3107.

Laakso, H., Aggson, T.L., Pfaff, R.F., Hanson, W.B., 1994. Downdrafting plasma flow in equatorial bubbles. J. Geophys. Res. 99, 11507–11515. https://doi.org/10.1029/93JA03169.

Martinis, C., Eccles, J.V., Baumgardner, J., Manzano, J., Mendillo, M., 2003. Latitude dependence of zonal plasma drifts obtained from dual-site airglow observations. J. Geophys. Res. Space Phys. 108 (A3), 1–10. https://doi.org/10.1029/2002JA009462.

Mcdonald, B.E., Ossakow, S.L., Zalesak, S.T., 1981. Scale sizes and lifetimes of f region plasma cloud striations as determined by the condition of marginal stability. J. Geophys. Res. 86 (1), 5775–5784.

Mendillo, M., Tyler, A.N.N., 1983. Geometry of depleted plasma regions in the equatorial ionosphere. J. Geophys. Res. 88 (3), 5778–5782.

Mukherjee, G.K., Carlo, L., Mahajan, S.H., Patil, P.T., 1998. First results of all-sky imaging from India. Earth Planets Space 50, 119–127.

Nade, D.P., Sharma, A.K., Nikte, S.S., Patil, P.T., Ghodpage, R.N., Rokade, M.V., Gurubaran, S., Taori, A., 2013. Zonal velocity of the equatorial plasma bubbles over Kolhapur, India. Ann. Geophys. 31 (11), 2077–2084. https://doi.org/10.5194/angeo-31-2077-2013.

Nade, D.P., Shetti, D.J., Sharma, A.K., Taori, A., Chavan, G.A., Patil, P. T., 2015. Geographical analysis of equatorial plasma bubbles by GPS and nightglow measurements. Adv. Space Res. 56 (9), 1901–1910. https://doi.org/10.1016/j.asr.2015.03.030.

Narayanan, V.L., Gurubaran, S., Emperumal, K., 2009. Imaging observations of upper mesospheric nightglow emissions from Tirunelveli (8.7°N). Indian J. Radio Space Phys. 38 (3), 150–158.

Narayanan, V.L., Gurubaran, S., Shiokawa, K., 2016a. Direct observational evidence for the merging of equatorial plasma bubbles. J. Geophys. Res.: Space Phys. 121, 7923–7931. https://doi.org/10.1002/2014JA020025.

Narayanan, V.L., Gurubaran, S., Shiokawa, K., Emperumal, K., 2016b. Shrinking equatorial plasma bubbles. J. Geophys. Res. Space Phys. 121 (7), 6924–6935. https://doi.org/10.1002/2016JA022633.

Narayanan, V.L., Gurubaran, S., Shiny, M.B.B., Emperumal, K., Patil, P. T., 2017. Some new insights of the characteristics of equatorial plasma bubbles obtained from Indian region. J. Atmos. Sol. Terr. Phys. 156, 80–86. https://doi.org/10.1016/j.jastp.2017.03.006.

Patra, A.K., Phanikumar, D.V., Pant, T.K., 2009. Gadanki radar observations of F region field-aligned irregularities during June solstice of solar minimum: first results and preliminary analysis. J. Geophys. Res. Space Phys. 114, 1–10. https://doi.org/10.1029/2009JA014437.

Patra, A.K., Srinivasulu, P., Chaitanya, P.P., Rao, M.D., Jayaraman, A., 2014. The ion temperature gradient: an intrinsic property of Earth’s magnetotail. J. Geophys. Res. Space Phys. 122 (8), 8295–8309. https://doi.org/10.1002/2017JA024209.

Pimenta, A.A.I., Fagundes, P.R., Bittencourt, J.A., Sahai, Y., Gobbi, D., Medeiros, A.F., Taylor, M.J., 2001. Ionospheric plasma bubble zonal drift: a methodology using OI 630 nm all-sky imaging systems. Adv. Space Res. 27, 1219–1224. https://doi.org/10.1016/S0273-1177(01)00201-0.

Sahai, Y., Abalde, J.R., Fagundes, P.R., Pillat, V.G., Bittencourt, J.A., 2006. First observations of detached equatorial ionospheric plasma depletions using OI 630.0 nm and OI 777.4 nm emissions nightglow imaging 33, 1–5. https://www.doi.org/10.1029/2005GL025262.

Sharma, A.K., Nade, D.P., Nikte, S.S., Ghodpage, R.N., Patil, P.T., Rokade, M.V., Vhatkar, R.S., 2012. Analysis of plasma bubbles observed in night airglow emission line OI 630.0 nm from Kolhapur using all sky imager Retrieved from. Issue Int. J. Eng. Sci. Res.-IJESR 03 (02), 746–750 <http://ijesr.in/>.

Sharma, A.K., Nade, D.P., Nikte, S.S., Ghodpage, R.N., Patil, P.T., Rokade, M.V., Vhatkar, R.S., Gurubaran, S., 2014. Development of fast image analysis technique for All-Sky images. Curr. Sci. 106 (8), 1085–1093.

Sharma, A.K., Gurav, O.B., Chavan, G.A., Gaikwad, H.P., Ghodpage, R.N., Patil, P.T., 2017. Variation in occurrence of equatorial plasma bubbles (EPBs) using All Sky Imager from low latitude station Kolhapur (16.8°N, 74.2°E). Adv. Space Res. 60 (11), 2452–2463. https://doi.org/10.1016/j.asr.2017.09.014.

Sharma, A.K., Gurav, O.B., Gaikwad, H.P., Chavan, G.A., Nade, D.P., Nikte, S.S., Ghodpage, R.N., Patil, P.T., 2018. Study of equatorial plasma bubbles using all sky imager and scintillation technique from Kolhapur station: a case study. Astrophys. Space Sci. 363, 83. https://doi.org/10.1007/s10509-018-3303-4.

Shiokawa, K., Otsuka, Y., Lynn, K.J.W., Wilkinson, P., Tsugawa, T., 2015. Airglow-imaging observation of plasma bubble disappearance at geomagnetically conjugate points. Earth Planets Space 67 (1). https://doi.org/10.1186/s40623-015-0202-6.

Taori, A., Sindhya, A., 2014. Measurements of equatorial plasma depletion velocity using 630 nm airglow imaging over a low-latitude Indian station. J. Geophys. Res.: Space Phys. 119 (1), 396–401. https://doi.org/10.1002/2013JA019465, 1–6.

Xiong, C., Xu, J., Wu, K., Yuan, W., 2018. Longitudinal thin structure of equatorial plasma depletions coincidently observed by Swarm constellation and all-sky imager. J. Geophys. Res. Space Phys. 123, 1593–1602. https://doi.org/10.1002/2017JA025091.

Yokoyama, T., Shinagawa, H., Jin, H., 2014. Nonlinear growth, bifurcation, and pinching of equatorial plasma bubble simulated by three-dimensional high-resolution bubble model. J. Geophys. Res. Space Phys. 119 (12), 10474–10482. https://doi.org/10.1002/2014JA020708.

Zalesak, S.T., Ossakow, S.L., Chaturvedi, P.K., 1982. Nonlinear equatorial spread F: The effect of neutral winds and background Pedersen conductivity. J. Geophys. Res 87, 151. https://doi.org/10.1029/93ja00762.